Available online at www.sciencedirect.com
SCIENCE DIRECT®
Journal of Chromatography B, 790 (2003) 99–114
JOURNAL OF CHROMATOGRAPHY B
www.elsevier.com/locate/chromb

# Hydrophobic interaction chromatography of proteins II. Binding capacity, recovery and mass transfer properties

Rainer Hahn, Karin Deinhofer, Christine Machold, Alois Jungbauer*

*Institute for Applied Microbiology, University of Agricultural Sciences, Muthgasse 18 A-1190 Vienna, Austria*

**Abstract**

Hydrophobic interaction chromatography media suited for large scale separations were compared regarding dynamic binding capacity, recovery and mass transfer properties. In all cases, pore diffusion was the rate limiting step. Reduced heights equivalent to a theoretical plate for bovine serum albumin derived from breakthrough curves at reduced velocities between 60 and 1500 ranged from 10 to 700. Pore diffusion coefficients were derived from pulse response experiments for the model proteins α-lactalbumin, lysozyme, β-lactoglobulin, bovine serum albumin and immunoglobulin G. Diffusivity of lysozyme did not follow the trend of decreasing diffusivity with increasing molecular mass, as observed for the rest of the proteins. In general, mass transfer coefficients were smaller compared to ion-exchange chromatography. Dynamic binding capacities for the model protein bovine serum albumin varied within a broad range. However, sorbents based on polymethacrylate showed a lower dynamic capacity than media based on Sepharose. Some sorbents could be clustered regarding binding capacity affected by salt. These sorbents exhibited a disproportional increase of binding capacity with increasing ammonium sulfate concentration. Recovery of proteins above 75% could be observed for all sorbents. Several sorbents showed a recovery close to 100%.


*Keywords:* Hydrophobic interaction chromatography; Pore diffusion; Mass transfer; Dynamic capacity; Binding studies; Proteins; Lactalbumins; Albumin; Lysozyme; Immunoglobulins

## 1. Introduction

Hydrophobic interaction chromatography (HIC) initially described by Shepard and Tiselius [1] is used for preparative and industrial scale purification of proteins [2,3]. Over the years a variety of HIC sorbents have been developed to fulfill the needs of different purifications [4–6]. From the large selection of ligands [7,8] only alkyl and aryl ligands are commonly used. Chain length and density of the hydrophobic ligands have been systematically varied and attached to agarose, dextran based media, polymethacrylate based media, coated silica and coated polystyrene [7,9]. Alkyl and aryl ligands have also been immobilized to the particle surface via a thioether bond [10]. The sulfur atom is responsible for a higher selectivity. Immunoglobulins have higher affinity to such sorbents than other serum proteins [11]. Proteins can be selectively desorbed from pyridyl derivatives sorbents by changing the pH of the buffer [5,12]. The base atoms play a crucial role, as according to the applied immobilization chemistry additional charged groups can be created [10], or electron donor–acceptor ligands can be introduced [13]. Also ligand density and ligand length have a

*Corresponding author. Fax: +43-1-369-7615.
*E-mail address:* jungbaue@hp01.boku.ac.at (A. Jungbauer).

1570-0232/02/$ – see front matter 
doi:10.1016/S1570-0232(03)00080-1

great impact on the property of an HIC sorbent [10,14]. Nowadays, sorbents with the same ligand length but different density are available [15]. Quantitative physical measurement of hydrophobicity of the porous surface has not yet been accomplished. Therefore the hydrophobic nature of the surface must be indirectly determined either by retention of reference proteins or by adsorption capacity. The adsorption is further influenced by the type of salt and salt concentration. Melander and Horváth [16,17] found that the relative retention ($k'$) is dependent on the surface tension increment unique for each type of salt and the concentration of the respective salt. Beside ligand length and density, the particle size and its porous structure influence adsorption. The pore size determines the effective ligand density, which is always lower than the nominal one. Particle size and pore structure such as length, radius, tortuosity and connectivity influence the mass transport.

Equilibrium and kinetic parameters for the adsorption of chymotrypsinogen on a hydrophobic silica sorbent have been published by Tongta et al. [18]. Conder and Hayek [19] investigated the adsorption characteristics of bovine serum albumin on a similar sorbent. In both cases batch adsorption in a stirred tank was carried out to follow the kinetics of adsorption. A broad overview of properties such as capacity, selectivity as well as mass transfer characteristics of different matrices is not available. Proteins may also undergo a conformational change and aggregation may occur upon adsorption and addition of high salt concentration [2,20]. Salt also effects the binding properties into mass transfer and recovery may decline.

Taking all these properties in account it is very difficult to compare the different sorbents with a single assay. Kasnäs et al. [21] applied principal component analysis (PCA) to data obtained from the elution position of proteins in descending salt gradients. Together with the protein hydrophobicity, charge, size and other properties, different classes of interaction and classes of media types could be classified. However, information on mass transfer properties was not included in this study. Multiple assays are required to address the most important properties for large scale application such as dynamic binding capacity, static binding capacity and mass transfer properties.

The dependence of the dynamic binding capacity (DBC) on the velocity is a central criterion for optimization, throughput, productivity and bed utilization [22]. In HIC, the dependence of DBC on the type and concentration of the salt comprises an additional dimension which must be considered. Plots of DBC versus both variables were constructed. From the shape of the breakthrough curve mass transport properties were derived. The number of transfer units were calculated and plotted against the reduced velocity. A high binding capacity is not beneficial if the protein cannot be easily eluted from the column, a phenomenon which is often attributed to HIC. Therefore we also investigated the recovery yield for two model proteins, bovine serum albumin (BSA) and ovalbumin, a hydrophilic protein.

In a previous study, we compared the selectivity of HIC sorbents by relating the relative retention of a set of model proteins to the ionic strength [23]. This was performed by pulse response experiments at different ammonium sulfate concentrations. In this paper we present an additional evaluation of these data.

## 2. Materials and methods

### 2.1. Materials

#### 2.1.1. Buffers and proteins

All buffer ingredients were from Merck (Vienna, Austria). The model proteins α-lactalbumin, β-lactoglobulin, bovine immunoglobulin (Ig) G, bovine serum albumin, ovalbumin, lysozyme and lactoferrin were purchased from Sigma–Aldrich (Vienna, Austria).

#### 2.1.2. Instrumentation

Pulse response and recovery experiments were performed on an ÄKTA-Explorer 100 system (Amersham Biosciences, Uppsala, Sweden) consisting of a compact separation unit and a personal computer running a control system (Unicorn, version 3.1). Experiments for determination of the dynamic binding capacity were performed on a fast protein liquid chromatography (FPLC) system equipped with a control system (FPLC director version 1.10).

*2.1.3. Stationary phases*

Phenyl Sepharose high-performance (HP), Phenyl Sepharose 6FF high substitution, Phenyl Sepharose 6FF low substitution, Octyl Sepharose 4FF, Butyl Sepharose 4FF, Hexyl-S-Sepharose 6FF, Butyl-S-Sepharose 6FF, Pyridyl-S-Sepharose 6FF, Methyl Sepharose 4FF Butyl Sepharose high-performance (HP), Source 15 Ether, Source 15 Isobutyl and Source 15 Phenyl were provided by Amersham Biosciences (Uppsala, Sweden). Toyopearl butyl 35 μm, Toyopearl butyl 65 μm, Toyopearl butyl 100 μm, Toyopearl phenyl 35 μm, Toyopearl phenyl 65 μm and Toyopearl phenyl 100 μm were purchased from TosoHaas (Stuttgart, Germany), Macro-Prep Methyl and Macro-Prep *t*-Butyl were purchased from Bio-Rad (Hercules, CA, USA). Poros 20 PE was purchased from Applied Biosystems (Vienna, Austria).

*2.2. Methods*

*2.2.1. Dynamic binding capacity*

HR 5 columns (I.D. 5 mm, Amersham Biosciences) were filled with approximately 1 ml sorbent and packed with a velocity of 1.5 ml/min. A 20-m*M* sodium phosphate buffer, pH 7.0 was prepared as elution buffer. The salt buffer was $(NH_4)2_SO_4$ at concentrations of 1.0, 1.2, 1.5 and 1.75 *M* dissolved in 20 m*M* sodium phosphate buffer, pH 7.0. Columns were regenerated with 2.5 ml 50% ethanol and then equilibrated with 3 ml salt buffer. Then the sample (BSA at 1 mg/ml) was loaded. Flow rates of 0.15, 0.33, 0.5, 0.65, 0.98 and 1.30 ml/min were tested. The amount of sample loaded varied between 25 and 110 ml. Buffers and samples were filtrated and degassed prior to chromatography. Data acquisition was performed with an automatically A/D converter (Analytical Series 900 from PE Nelson System, Cupertino, CA, USA). The digital data were transferred into an ASCII format and further processed with Computer program SigmaPlot 7.0 (SPSS, Erkrath, Germany). The dynamic binding capacity was determined at 2.5% breakthrough.

*2.2.2. Recovery*

A feed with 1 mg/ml BSA and 1 mg/ml ovalbumin corresponding to 70% of DBC was loaded onto the HIC columns, HR 5 columns with approximately 1 ml of sorbent. The proteins were dissolved and loaded in 1, 1.5 and 1.75 *M* ammonium sulfate. Elution was carried out with a buffer of low ionic strength, 20 m*M* sodium phosphate. The remaining sample was removed with 30% isopropanol for the determination of recovery. In the case of unspecific adsorbed molecules, the recovery is less than 100%. After equilibration of the column for 10 column volumes (CVs) with the corresponding ammonium sulfate buffer, the sample was applied at a flow-rate of 0.33 ml/min. Unbound protein was eluted by a washing out step with ammonium sulfate buffer at a flow-rate of 0.5 ml/min. Then the column was switched into the bypass position and the system was flushed with sodium phosphate buffer for 15 ml. The column was switched back and elution was carried out with sodium phosphate buffer at a flow-rate of 0.33 ml/min for 5 ml. 4 ml isopropanol was applied to the column to elute the unspecific bound protein. Fractions obtained with sodium phosphate buffer and isopropanol were collected separately with a fraction collector and the protein content was measured with a two channel photometer at a wavelength of 280 nm.

The recovery was calculated by following equation:

$$\text{Recovery} = \frac{q_{\text{initial}} + q_{\text{elution}}}{q_{\text{regenerate}}} \cdot 100 \quad (1)$$

where $q_{\text{initial}}$ is the mass of loaded protein, $q_{\text{elution}}$ the protein in the eluate and $q_{\text{regenerate}}$ the mass of protein in the regenerate.

*2.2.3. Isocratic runs*

2 ml of each sorbent were filled into HR5/10 columns (Amersham Biosciences) and packed at a flow velocity of 450 cm/h. The bed volume varied between 1.8 and 2 ml.

A 20-m*M* sodium phosphate buffer, pH 7.0 was prepared as elution buffer. The salt buffer was $(NH_4)_2SO_4$ at various concentrations dissolved in 20 m*M* sodium phosphate buffer, pH 7.0. The buffers were filtrated and degassed prior to chromatography. Isocratic runs were designed as follows: After equilibration of the columns (3 CVs) at a flow velocity of 306 cm/h with $(NH_4)_2SO_4$ buffer of desired molarity, a 50-μl pulse of the protein sample was injected. The elution volume was 6 CVs at a linear flow velocity of 100 cm/h. Regeneration was

effected with 20 m*M* sodium phosphate buffer, pH 7.0. The desired salt concentration in the eluent buffer was obtained by mixing 1.0 *M* $(NH_4)_2SO_4$ with 20 m*M* sodium phosphate pH 7.0. The proteins were dissolved in the respective buffer with ammonium sulfate. Final protein concentration was 5 mg/ml for ovalbumin, 3 mg/ml for α-lactalbumin and BSA and 2 mg/ml for IgG, lactoglobulin, lactoferrin and lysozyme.

## 3. Theory

### 3.1. Frontal analysis

Dispersion parameters were derived from breakthrough curves as described by Rosenberg [24] and Lettner et al. [25]. The breakthrough curve can be considered as the integral of a Gaussian normal distribution curve thus the number of plates can be calculated from a normalized response curve as:

$$N = \frac{t_{0.5}^2}{(t_{0.5} - t_{0.15})^2} \tag{2}$$

where $t_{0.5}$ is the time at 50% of the relative response and corresponds to the point of inflection. $t_{0.5} - t_{0.15}$ corresponds to $\sigma$.

### 3.2. Pulse response experiments

The plate height of a given solute and column can be related to physical parameters by the van Deemter equation which can be written as [26]:

$$\mathrm{HETP} = \frac{2D_L}{u} + \frac{2\epsilon u}{1-\epsilon} \cdot \left(\frac{k'}{1+k'}\right)^2 \left[\frac{r_p}{3k_f} + \frac{r_p^2}{15\epsilon_p D_p} + \frac{\rho_p K}{(\epsilon_p + \rho_p K)^2} \cdot \frac{r_s^2}{15 D_s}\right] \tag{3}$$

where HETP = height equivalent to a theoretical plate. The symbols are defined in Section 5.

According to Sherwood et al. [27] we define an pore diffusion mass transfer coefficient:

$$k_p = \frac{10 D_p}{d_p} \tag{4}$$

which lumps together pore diffusion and the kinetics of adsorption and desorption. Under the experimental conditions the contribution from mobile phase diffusion can be neglected (first term of square bracket) and surface diffusion (last term of square bracket) is unlikely to be dominant for the chosen sorbents. Thus we may rewrite the plate height equation in reduced form by dividing with $d_p$ and inserting Eq. (4). After rearranging we get:

$$h = \frac{2D_L}{d_p u} + \frac{\epsilon u}{1-\epsilon} \cdot \left(\frac{k'}{1+k'}\right)^2 \cdot \left(\frac{1}{3\epsilon_p k_p}\right) \tag{5}$$

This equation was used to fit data from pulse response experiments.

## 4. Results and discussion

Only HIC sorbents suited for large scale separation of proteins were selected for this comparative study. Information on ligand length, density and particle size are listed in Table 1. In order to compare the dynamic binding capacity (DBC), breakthrough curves (BTCs) with BSA were performed at different velocities (50, 100, 150, 200, 300 and 400 cm/h) and ammonium sulfate concentrations (1.0, 1.2, 1.5 and 1.75 *M*). Other salt types were not investigated since it is clear that the surface tension increments determine the binding strength [16]. BTCs for two different salt concentrations, 1.0 and 1.75 *M*, are shown in Fig. 1. Remarkable differences in shape of the breakthrough curves can be observed.

As expected, sorbents with small particle diameter exhibit sharp breakthrough and velocity did not effect the binding capacity. Influence of velocity and salt concentration in the running buffer on DBC is shown in Fig. 2. DBC was determined at 2.5% breakthrough. Butyl Sepharose HP showed highest DBC. In contrast, all polymethacrylate sorbents exhibited relative low capacity. Influence of velocity on DBC was less pronounced compared to the Sepharose based media.

When DBC is plotted versus salt concentration in the eluent, sorbents can be grouped in several classes (Fig. 3). The custom designed media Hexyl-S-Sepharose 6FF, Methyl Sepharose 4FF, Pyridyl-S-

Table 1
Properties of selected sorbents according to the manufacturers (n.a. not available)

| Sorbent | Base matrix | Ligand type | Ligand substitution (μmol/ml gel) | Mean particle size (μm) |
|---|---|---|---|---|
| Phenyl Sepharose High Performance | Crosslinked agarose 6% | Phenyl | 25 | 34 |
| Phenyl Sepharose 6FF low substitution | Crosslinked agarose 6% | Phenyl | 20 | 90 |
| Phenyl Sepharose 6 FF high substitution | Crosslinked agarose 6% | Phenyl | 40 | 90 |
| Butyl Sepharose 4 FF | Crosslinked agarose 4% | Butyl | 50 | 90 |
| Octyl Sepharose 4 FF | Crosslinked agarose 4% | Octyl | 5 | 90 |
| Toyopearl Phenyl 100 μm | Polymethacrylate | Phenyl | n.a. | 100 |
| Toyopearl Phenyl 65 μm | Polymethacrylate | Phenyl | n.a. | 65 |
| Toyopearl Phenyl 35 μm | Polymethacrylate | Phenyl | n.a. | 35 |
| Toyopearl Butyl 100 μm | Polymethacrylate | Butyl | n.a. | 100 |
| Toyopearl Butyl 65 μm | Polymethacrylate | Butyl | n.a. | 65 |
| Toyopearl Butyl 35 μm | Polymethacrylate | Butyl | n.a. | 35 |
| Toyopearl Etherl 65 μm | Polymethacrylate | Hydroxy | n.a. | 65 |
| Hexyl-S Sepharose 6FF | Crosslinked agarose 6% | S-hexyl | 8 | 90 |
| Methyl Sepharose 4 FF | Crosslinked agarose 4% | Methyl | n.a. | 90 |
| Pyridyl-S Sepharose 6FF | Crosslinked agarose 6% | S-pyridyl | n.a. | 90 |
| Butyl-S Sepharose 6 FF | Crosslinked agarose 6% | S-butyl | n.a. | 90 |
| Butyl Sepharose HP | Crosslinked agarose 6% | Butyl | n.a. | 34 |
| Macroprep Methyl | Polymethacrylate | Methyl | n.a. | 50 |
| Macroprep *t*-Butyl | Polymethacrylate | *t*-butyl | n.a. | 50 |
| Poros PE 20 | Polystyrene–divinylbenzene | Phenyl | n.a. | 20 |
| Source 15 Phenyl | Polystyrene–divinylbenzene | Phenyl | n.a. | 15 |
| Source 15 Isobutyl | Polystyrene–divinylbenzene | *t*-butyl | n.a. | 15 |
| Source 15 Ether | Polystyrene–divinylbenzene | Hydroxy | n.a. | 15 |

Sepharose 6FF, Butyl-S-Sepharose 6FF and Butyl Sepharose HP exhibit a disproportional increase in DBC with salt, while for others a quasi linear increase can be observed. Within a concentration range window of 0.5 *M* ammonium sulfate up to 10-fold higher capacity can be achieved. Such a behavior might be explained by induction of preferred aggregation upon surface contact, unfolding or multilayer formation. Precipitation of protein on the surface is not likely to have been occurred, since recovery of adsorbed protein was fairly high (see Table 3). Precipitated protein would be difficult to remove from the column and pressure drop would also increase. Both effects have not been observed. Further investigations are necessary to explain this behavior but did exceed the scope of the study.

Then it was attempted to quantify the shape of the BTC regarding mass transfer. Approximation of BTC by the Thomas model [28] or other models were not applicable since the curves could not be approximated. In addition, isotherms may significantly deviate from the Langmuir type. Conder and Hayek [19] observed a BET II type isotherm for adsorption of BSA onto a porous silica matrix functionalized with a propyl ligand. The deviation of pure sigmoidal BTC was observed mainly at higher salt concentrations.

The plate number was determined from the BTCs according to Lettner et al. [25] and the reduced HETP was plotted against the reduced velocity ($\mathrm{ReSc} = ud_\mathrm{p}/D_\mathrm{m}$). This plot represents the width of the mass transfer zone normalized to the particle diameter as a function of the velocity and the protein diffusivity (Fig. 4). When proteins are separated by HIC the influence of the ammonium sulfate concentration on the mass transfer properties must also be addressed. In combination with the dynamic binding capacity it may help to determine an optimal operational range for a specific purification problem, because the breakthrough curves may become very broad with increasing salt concentration. With the investigated sorbents this was not the case. BTCs of Source 15 and some Toyopearl sorbents at 1.0 *M* ammonium sulfate were not evaluated. Due to the early breakthrough the measured HETP values were rather imprecise. Dead time could not be measured

A

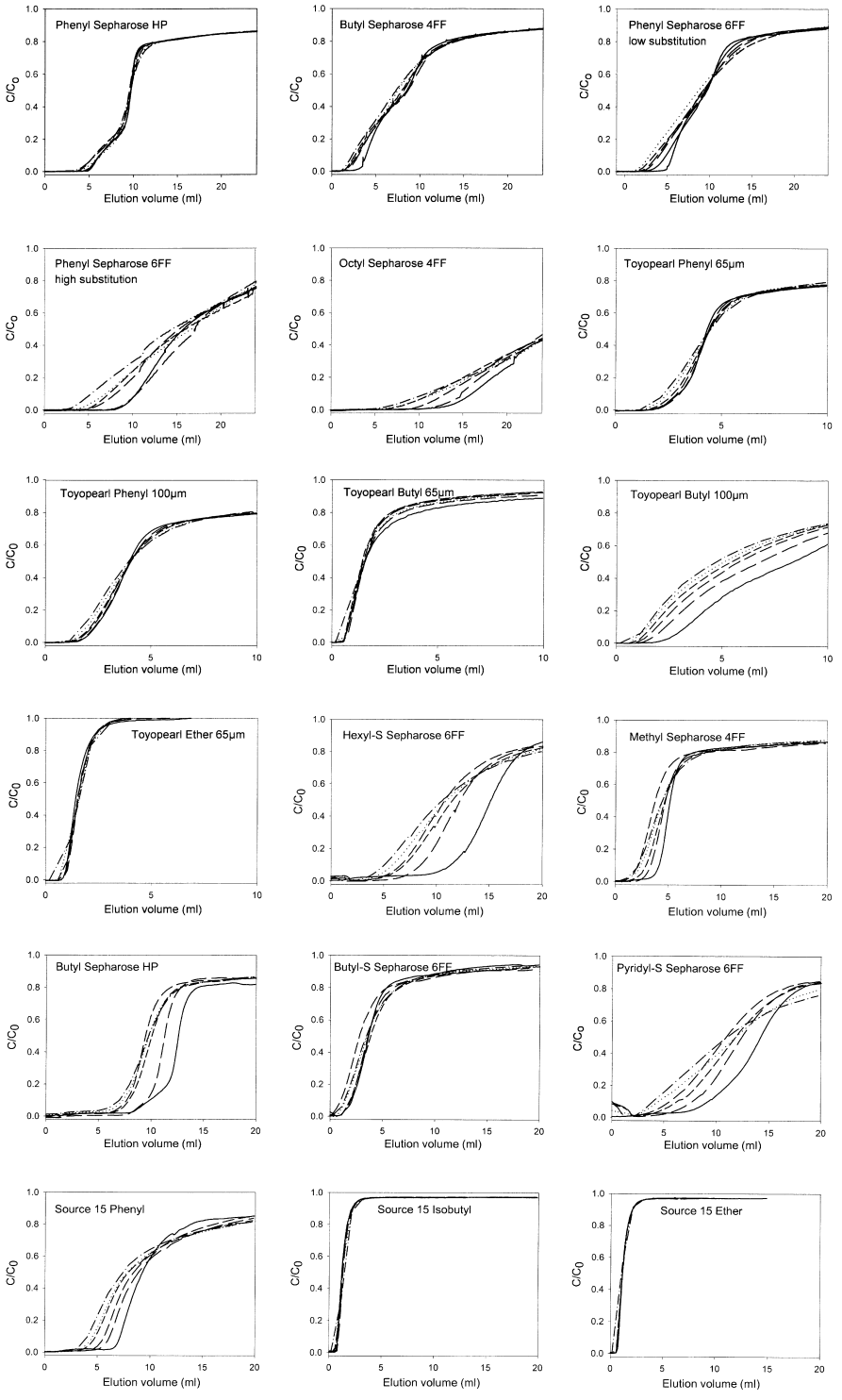


Fig. 1. Breakthrough curves with 1 mg/ml BSA on different HIC sorbents at different linear flow velocities and ammonium sulfate concentrations: (—) 50 cm/h; (— — ) 100 cm/h; (– –) 150 cm/h; (- - -) 200 cm/h; () 300 cm/h; (– – –) 400 cm/h. (A) 1.0 *M* ammonium sulfate; (B) 1.75 *M* ammonium sulfate.

B

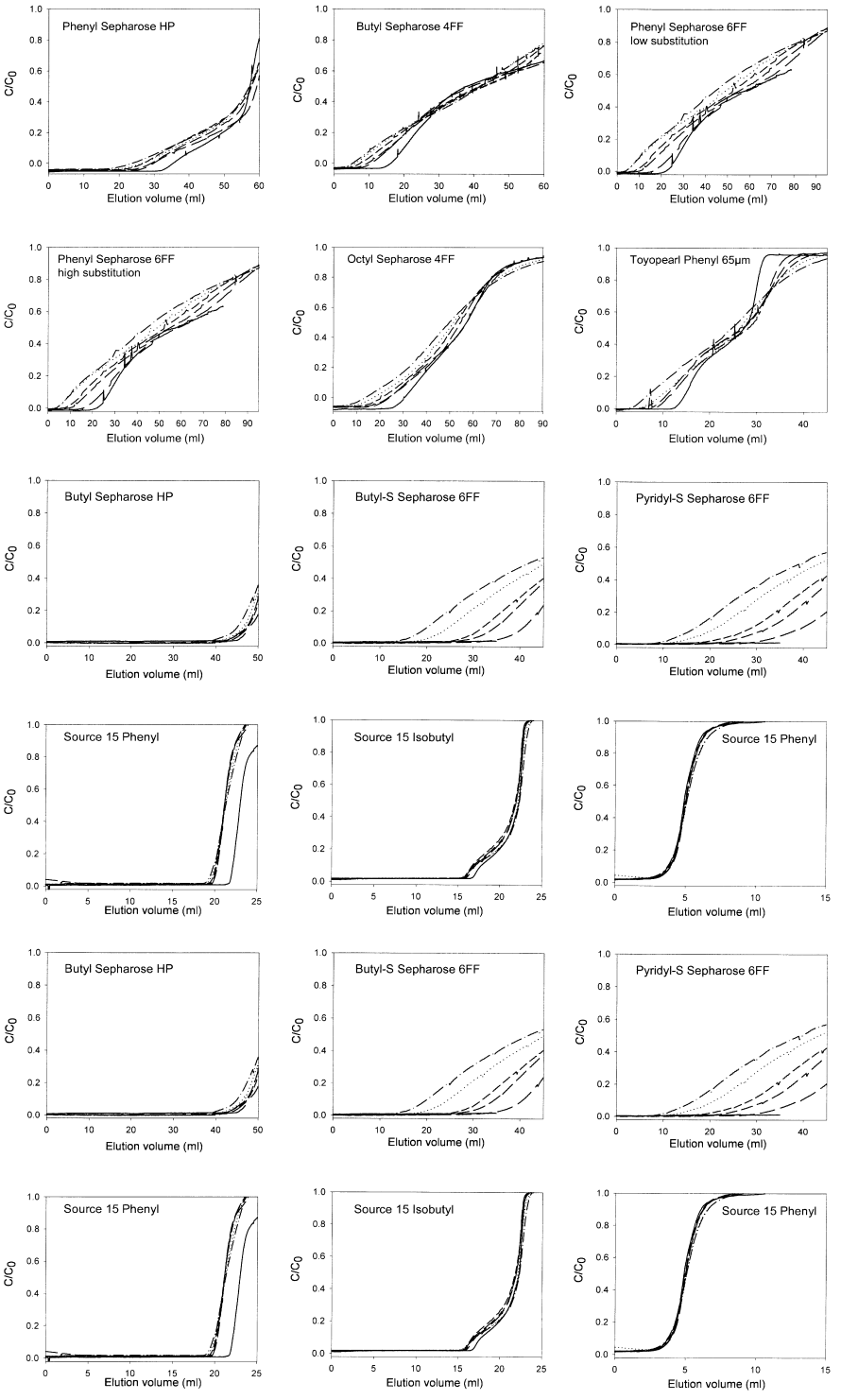


Fig. 1. (*continued*)

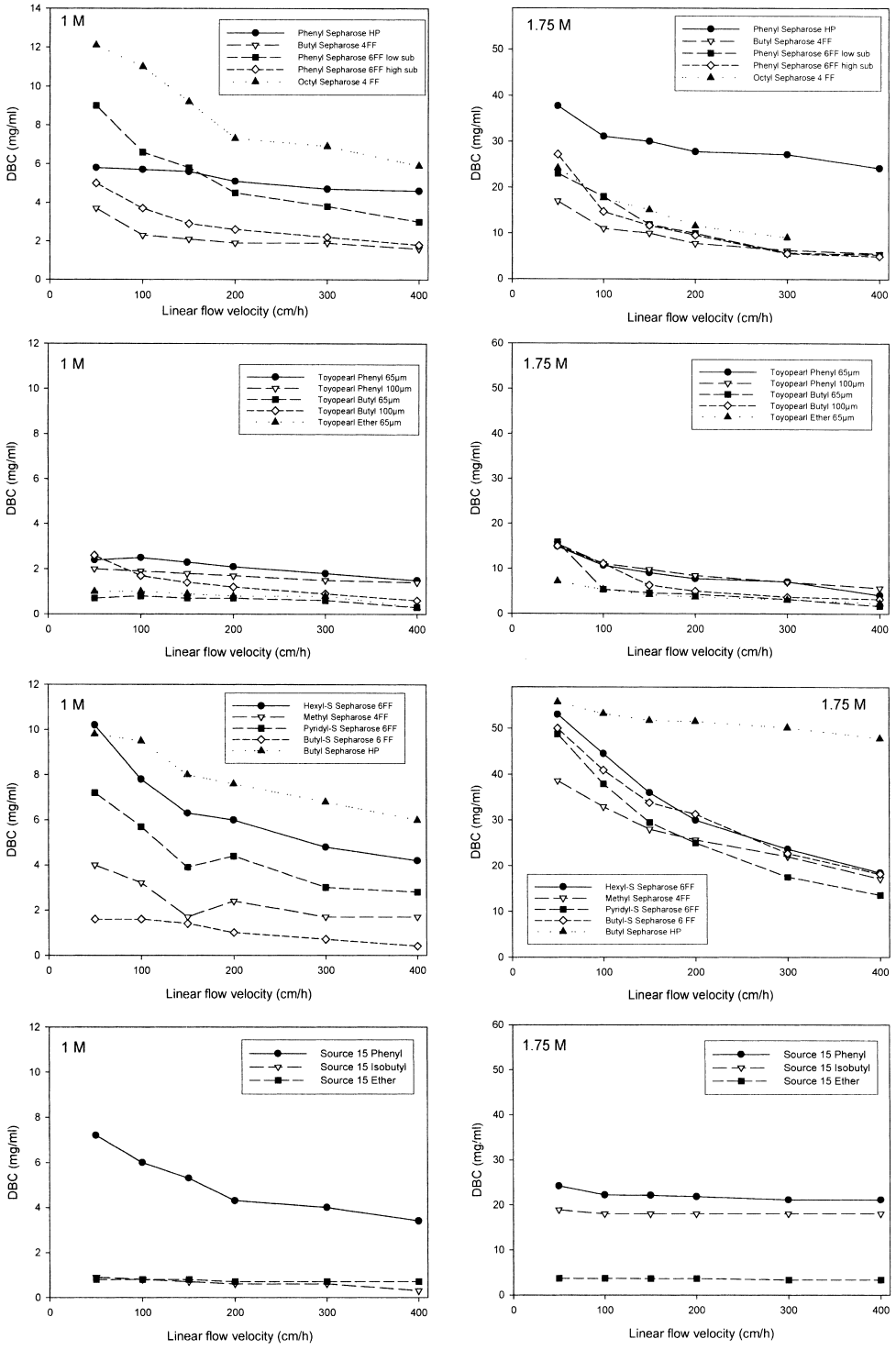


Fig. 2. Dynamic binding capacity dependent on the linear flow velocity at ammonium sulfate concentrations of 1.0 and 1.75 *M*, respectively.

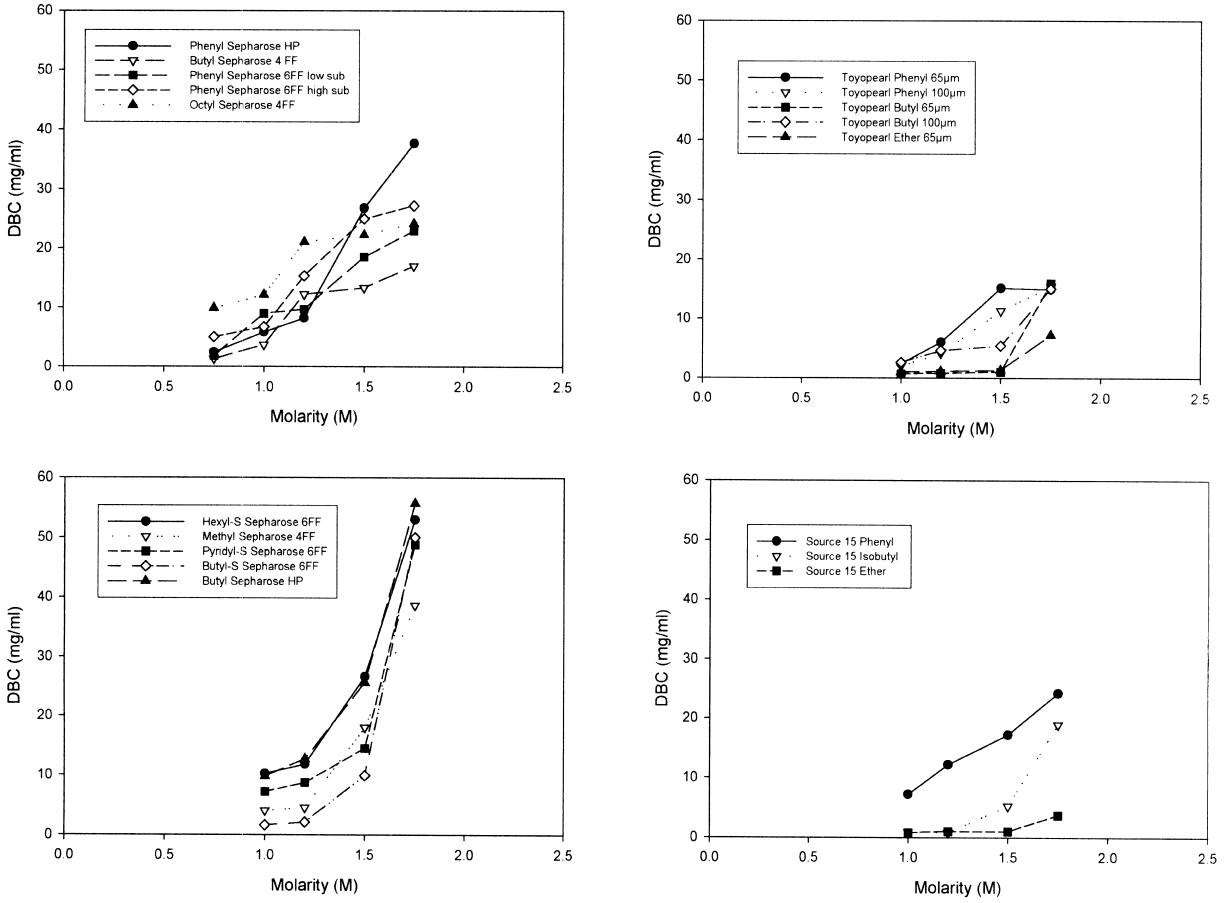


Fig. 3. Dynamic binding capacity dependent on the ammonium sulfate concentration in the loading buffer. Data were calculated from breakthrough curves performed at a linear flow velocity of 50 cm/h as shown in Fig. 1.

accurately enough. In all cases a strong pore diffusion control has been observed as reflected by the reduced HETP. According to LeVan et al. [26], at reduced velocities of $10^2$–$10^3$ and a reduced HETP between 10 and 700 pore diffusion is the controlling mechanism. These findings are in agreement with Tongta et al. [18]. They investigated a silica based material with chymotrypsinogen as model protein and the calculated kinetic parameters suggested pore diffusion control. Condor and Hayek [19] found similar results with BSA. In contrast to our experiments they extracted the kinetic parameters from batch adsorption experiments. The strong pore diffusion control dictates a careful optimization of feed concentration, velocity and column height during scale up.

In a previous study, we compared the selectivity of HIC sorbents by relating the relative retention of a set of model proteins to the ionic strength in the running buffer [23]. This was performed by pulse response experiments at different ammonium sulfate concentrations. The data from pulse response experiments can be also used to evaluate mass transfer properties under linear conditions. The peak width was determined by fitting the peak profiles with an exponential modified Gauss (EMG) function and the first and second peak moment were derived. The plate height was calculated from the moments and related to the normalized retention ($k'$). A modified van Deemter equation (Eq. (5)) was applied to extract a pore diffusion mass transfer coefficients ($k_p$). As an example the fit of IgG injected on

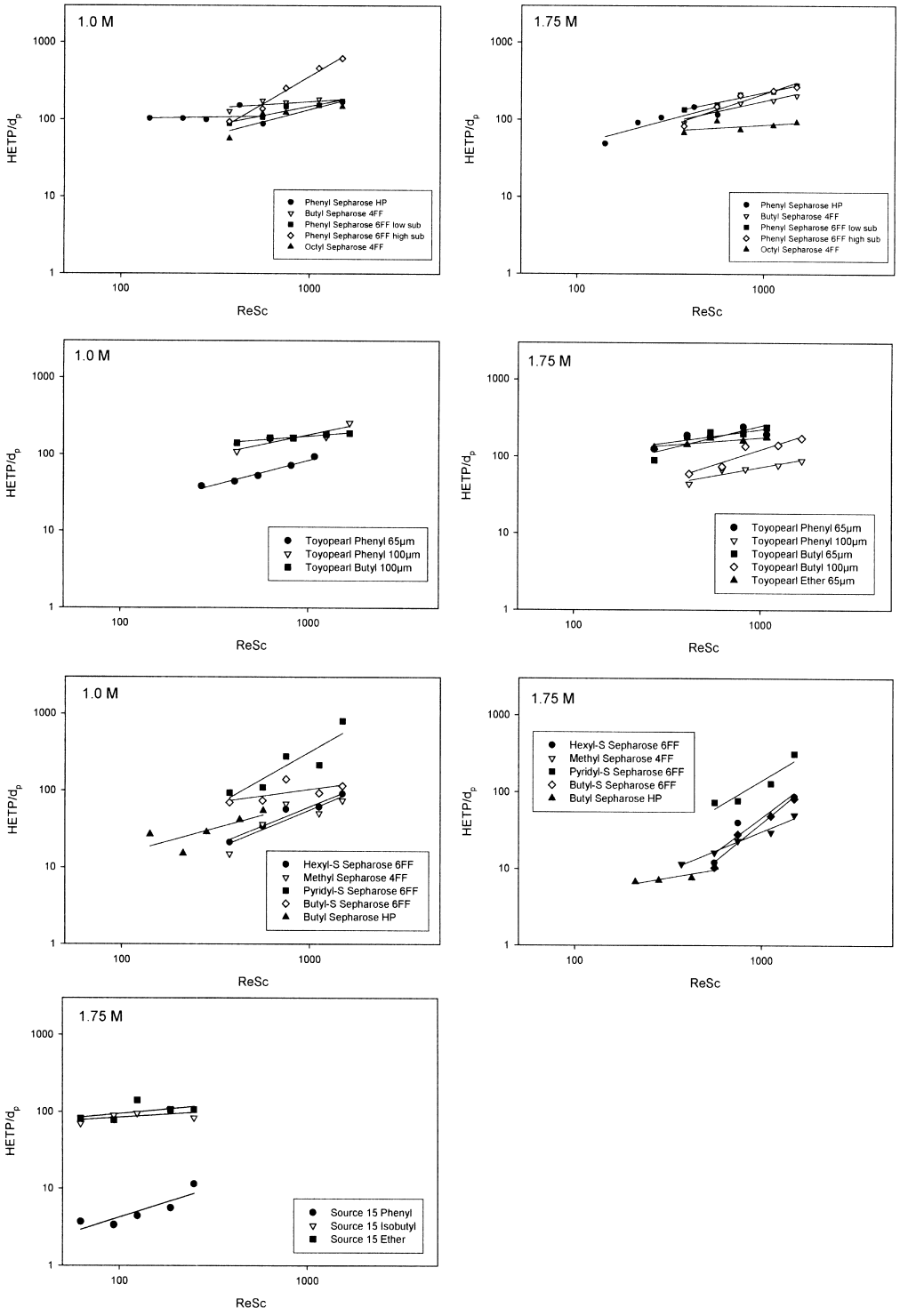


Fig. 4. Reduced HETP derived from breakthrough curves with 1 mg/ml BSA at ammonium sulfate concentrations of 1.0 and 1.75 M.

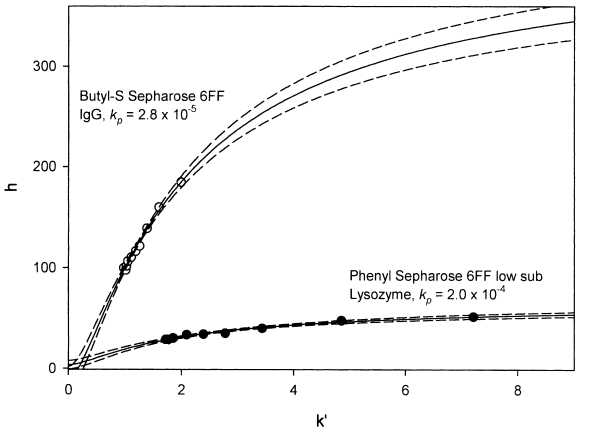


Fig. 5. Plots of reduced HETP versus retention factor derived from pulse response experiments. Data were fitted with Eq. (5) (solid lines). Dashed line represent the 95% confidence limits.

Butyl-S Sepharose and lysozyme on Phenyl Sepharose low sub are shown in Fig. 5. The latter one represents fast mass transfer while the first is typical for slow mass transfer. $k_p$ values calculated in such a way have not been published for HIC sorbents. The $k_p$ values lump together pore diffusion and adsorption kinetics and neglect film diffusion. We assume that slow binding or conformational changes upon adsorption significantly contributes to the overall mass transfer rate. The experiments with BTCs corroborate that pore diffusion resistance and the adsorption kinetics are the rate limiting steps. Diffusivities were calculated by Eq. (4) as $D_p = k_p d_p / 10$ [27]. The results are summarized in Fig. 6 and Table 2

For ion-exchange chromatography diffusivity values derived from pulse response experiments are available [29], but not for HIC. We observed lower diffusivity values for HIC than reported for ion-exchange (IEX) chromatography. Our model proteins used for the investigation had a similar molecular mass as the proteins used in the study of IEX. Higher diffusivities can be explained by the long range forces acting on proteins in IEX, pulling proteins into the pores. In general, diffusivities derived from pulse response experiments were larger compared to these from batch adsorption. Under non-linear conditions, other effects may decelerate the diffusion process. With increasing salt concentration the size of the molecules increases and aggregation may occur [2,19]. The applied model does not consider these effects. Our calculated values for HIC sorbents based on pulse response experiments are larger indicating faster mass transfer. The approximated data for $k_p$ values depend also on the quality of the fit of the peak, especially at higher salt concentrations broad and tailed peaks have to be handled. Despite this problem this is a fast way to get information on mass transfer properties with a reasonable amount of material and experimental efforts, but on the expense of accuracy. To obtain a similar information as shown in Fig. 6, 80 batch

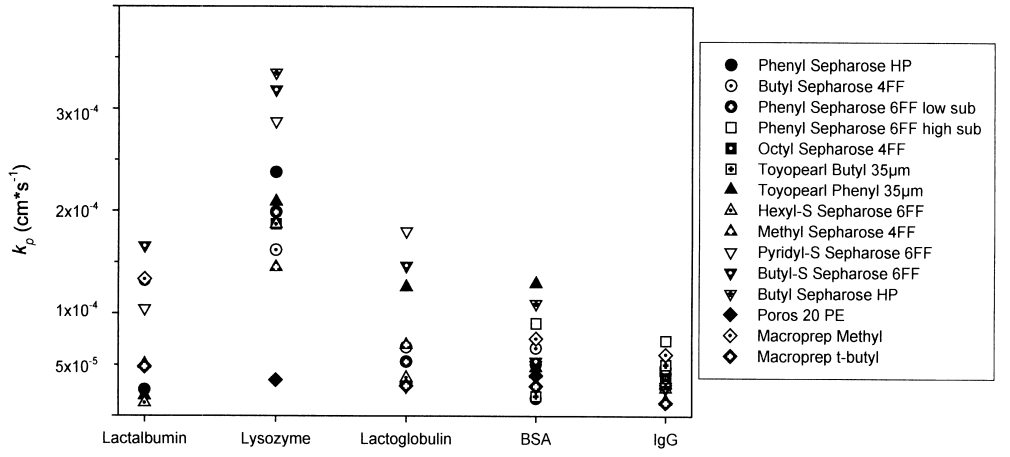


Fig. 6. Pore diffusion coefficients for the model proteins lactalbumin ($M_r$ = 14 200), lysozyme ($M_r$ = 14 400), lactoglobulin ($M_r$ = 18 400), BSA ($M_r$ = 66 000), and IgG ($M_r$ = 150 000) calculated from Eq. (5).

Table 2
Pore diffusion coefficients $k_p$, pore diffusivities $D_p$ and ratio of pore diffusivities to the molecular diffusivity in free solution for lactalbumin, lysozyme, lactoglobulin, BSA and IgG

| | Lactabumin | | | | Lysozyme | | | | Lactoglobulin | | | |
|---|---|---|---|---|---|---|---|---|---|---|---|---|
| | $k_p$ ($10^{-5}$ cm/s) | Std. error ($10^{-5}$ cm$^2$/s) | $D_p$ ($10^{-8}$ cm$^2$/s) | $D_p/D_m$ ($10^{-2}$) | $k_p$ ($10^{-5}$ cm/s) | Std. error ($10^{-5}$ cm$^2$/s) | $D_p$ ($10^{-8}$ cm$^2$/s) | $D_p/D_m$ ($10^{-2}$) | $k_p$ ($10^{-5}$ cm/s) | Std. error ($10^{-5}$ cm$^2$/s) | $D_p$ ($10^{-8}$ cm$^2$/s) | $D_p/D_m$ ($10^{-2}$) |
| Phenyl Sepharose HP | 2.55 | 0.25 | 0.86 | 0.78 | 23.77 | 0.96 | 8.08 | 7.30 | 3.17 | 0.28 | 1.08 | 1.05 |
| Butyl Sepharose 4 FF | 13.24 | 1.26 | 11.88 | 8.36 | 16.16 | 1.03 | 14.55 | 13.05 | 6.74 | 2.64 | 6.07 | 5.93 |
| Phenyl Sepharose low subst. | | | | | 19.86 | 1.04 | 17.88 | 16.03 | 5.33 | 0.65 | 4.79 | 4.69 |
| Phenyl Sepharose high subst. | | | | | 9.09 | 0.69 | 8.19 | 7.34 | | | | |
| Octyl Sepharose 4 FF | | | | | 18.73 | 3.25 | 16.85 | 15.11 | | | | |
| Toyopearl Butyl 35 μm | | | | | | | | | | | | |
| Toyopearl Butyl 65 μm | | | | | | | | | | | | |
| Toyopearl Phenyl 35 μm | 1.95 | 0.31 | 0.68 | 0.62 | 20.88 | 3.83 | 7.30 | 6.56 | 12.60 | 1.85 | 4.41 | 4.31 |
| Hexyl-S Sepharose 6 FF | 1.26 | 0.23 | 1.14 | 1.02 | 18.71 | 1.98 | 16.84 | 15.10 | 3.76 | 0.24 | 3.39 | 3.51 |
| Methyl Sepharose 4 FF | 5.05 | 0.91 | 4.55 | 4.10 | 14.50 | 1.25 | 13.05 | 11.70 | 6.99 | 0.43 | 6.29 | 6.14 |
| Pyridyl-S Sepharose 6 FF | 10.43 | 1.17 | 9.39 | 8.46 | 18.55 | 3.29 | 25.80 | 23.20 | 18.00 | 3.35 | 16.22 | 15.86 |
| Butyl-S Sepharose 6FF | 16.56 | 1.07 | 14.91 | 13.43 | 31.83 | 2.94 | 28.65 | 25.69 | 4.84 | 0.86 | 4.35 | 4.25 |
| Butyl-S Sepharose HP | | | | | 33.50 | 5.10 | 11.39 | 10.21 | 2.89 | 0.28 | 0.98 | 9.60 |
| Porus 20 PE | | | | | 3.52 | 0.42 | 0.70 | 0.63 | | | | |
| Marcrprep Methyl | 13.32 | 3.23 | 6.66 | 5.97 | | | | | | | | |
| Marcoprep *t*-Butyl | 4.83 | 0.76 | 2.42 | 2.17 | | | | | 2.97 | 0.79 | 1.48 | 1.45 |

| | BSA | | | | IgG | | | |
|---|---|---|---|---|---|---|---|---|
| | $k_p$ ($10^{-5}$ cm/s) | Std. error ($10^{-5}$ cm$^2$/s) | $D_p$ ($10^{-8}$ cm$^2$/s) | $D_p/D_m$ ($10^{-2}$) | $k_p$ ($10^{-5}$ cm/s) | Std. error ($10^{-5}$ cm$^2$/s) | $D_p$ ($10^{-8}$ cm$^2$/s) | $D_p/D_m$ ($10^{-2}$) |
| Phenyl Sepharose HP | 1.72 | 0.41 | 0.58 | 0.87 | 4.17 | 2.28 | 1.42 | 2.78 |
| Butyl Sepharose 4 FF | 6.64 | 4.52 | 5.98 | 8.95 | 4.72 | 0.50 | 4.25 | 8.36 |
| Phenyl Sepharose low subst. | 5.07 | 0.85 | 4.56 | 6.83 | 2.85 | 0.23 | 5.56 | 5.04 |
| Phenyl Sepharose high subst. | | | | | 7.41 | 0.23 | 6.67 | 13.12 |
| Octyl Sepharose 4 FF | | | | | 3.76 | 0.80 | 3.38 | 6.65 |
| Toyopearl Butyl 35 μm | 1.95 | 0.87 | 0.69 | 1.02 | 5.06 | 0.35 | 1.77 | 3.48 |
| Toyopearl Butyl 65 μm | | | | | 4.68 | 0.57 | 3.04 | 5.98 |
| Toyopearl Phenyl 35 μm | 12.97 | 1.51 | 4.54 | 6.79 | 1.52 | 0.08 | 0.53 | 1.05 |
| Hexyl-S Sepharose 6 FF | 4.17 | 0.63 | 3.75 | 5.61 | 2.69 | 0.34 | 2.43 | 4.78 |
| Methyl Sepharose 4 FF | 4.76 | 0.69 | 4.29 | 6.42 | 3.15 | 0.27 | 2.84 | 5.58 |
| Pyridyl-S Sepharose 6 FF | 5.06 | 0.69 | 4.56 | 6.82 | | | | |
| Butyl-S Sepharose | 5.38 | 0.44 | 4.84 | 7.25 | 2.77 | 0.09 | 2.50 | 4.91 |
| Butyl Sepharose HP | 10.99 | 1.57 | 3.73 | 5.59 | 2.95 | 0.40 | 1.00 | 1.98 |
| Poros 20 PE | 2.87 | 0.82 | 0.57 | 0.86 | | | | |
| Macrprep Methyl | 7.58 | 1.20 | 3.79 | 5.67 | 6.04 | 0.90 | 3.02 | 5.94 |
| Macroprep *t*-Butyl | 2.93 | 0.66 | 1.47 | 2.19 | 1.31 | 0.17 | 0.65 | 1.28 |

uptake experiments would have been necessary, consuming much more material. In Fig. 6 effective mass transfer coefficients for five model proteins are shown. $k_p$ values decrease with molecular mass except for lysozyme. With lysozyme [23,30,31] additional electrostatic interactions were made responsible for the strong retention at low ionic strength. Sufficient salt was present to suppress such electrostatic interaction, therefore this effect can be excluded. Experiments where this phenomenon occurred were not taken for the calculation of diffusivities. It might be that lysozyme is much more compact than the other proteins. Lactalbumin aggregates when it gets adsorbed, this would be reflected by the low $k_p$ value. Benedek [32] has shown that lactalbumin undergoes conformational changes upon adsorption. From pulse response experiments we got some indications that conformational interconversion may take place. Peak deformation occurred in a characteristic manner as observed for Damkohler numbers between 1 and 10 [2]. The Damkohler number represents the ratio of the residence time in the column and the reaction time, in this case conformational interconversion. Partial unfolding such as global folding, *cis-trans* prolyl-peptidyl isomerization or intermediate formation takes place within a time span ranging from several seconds to minutes, that is the same time domain as the chromatography run.

It is also important to which extent proteins can be recovered after adsorption. To investigate protein recovery, BSA and ovalbumin were loaded to reach 70% of DBC. After a washing step, the protein was eluted by a low ionic strength buffer and the column was regenerated with 30% isopropanol. A representative chromatogram is shown in Fig. 7. Recovery was calculated by Eq. (1). Results are summarized in Table . For almost all sorbents a fairly high recovery above 90% was observed. Recovery above 100% was due to experimental error because small liquid samples with a high density had to be collected. Recovery was much better than generally assumed for HIC.

The presented data may serve as a rough guidance to select a certain HIC sorbent for a given separation problem. Especially when biospecific interaction is occurring, for instance between a hexyl-ligand and BSA, which has a binding pocket for fatty acids, the reported values in this paper are not representative for sole hydrophobic interaction. The presented

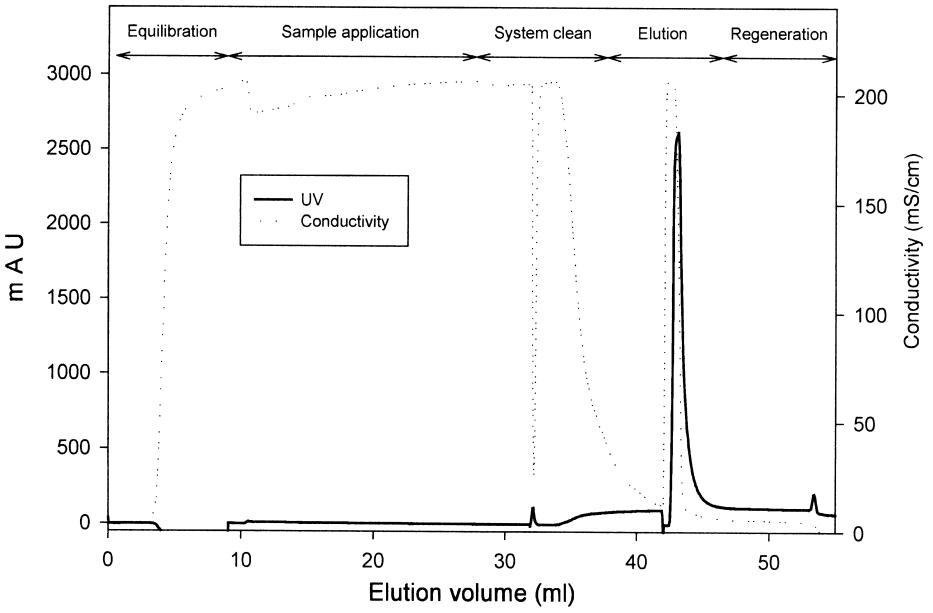


Fig. 7. Representative chromatogram for recovery experiments.

Table 3
List of recovery data for BSA and ovalbumin

| | Total protein (mg) | Eluate (mg) | Regenerate (mg) | Recovered protein (mg) | Total recovery (%) |
|---|---|---|---|---|---|
| BSA 1 M | | | | | |
| Phenyl Sepharose HP | 3.9 | 2.5 | 1.1 | 3.6 | 92.3 |
| Phenyl Sepharose high sub | 6.3 | 4.5 | 1.4 | 5.9 | 93.7 |
| Phenyl Sepharose low sub | 2.4 | 2.3 | 0.1 | 2.4 | 98.8 |
| Butyl Sepharose 4 FF | 1.6 | 1.5 | 0 | 1.5 | 90.6 |
| Octyl Sepharose FF | 7.2 | 5.3 | 1.7 | 7.0 | 97.6 |
| Toyopearl Butyl 100 μm | 2.0 | 1.1 | 0.6 | 1.7 | 84.2 |
| Butyl-S-Sepharose 6 FF | 1.1 | 0.34 | 0.0 | 1.06[a] | 96.4 |
| Butyl Sepharose HP | 6.7 | 6.0 | 0 | 6.0 | 89.9 |
| Source 15 PHE | 5.2 | 4.1 | 1.4 | 5.5 | 106.7 |
| BSA 1.5 M | | | | | |
| Phenyl Sepharose HP | 15.1 | 15.6 | 2.3 | 17.9 | 118.5 |
| Phenyl Sepharose high sub | 11.0 | 8.8 | 3.3 | 12.1 | 110 |
| Phenyl Sepharose low sub | 9.3 | 8.3 | 1.0 | 9.3 | 100.0 |
| Butyl Sepharose 4 FF | 7.2 | 7.14 | 0.02 | 7.16 | 99.4 |
| Octyl Sepharose FF | 13.9 | 14.7 | 0.3 | 15.0 | 107.9 |
| Toyopearl Butyl 100 μm | 5 | 3.9 | 1.1 | 5.0 | 100.0 |
| Hexyl-S-Sepharose 6 FF | 18.8 | 18.3 | 0.6 | 18.9 | 100.4 |
| Methyl Sepharose 4 FF | 12.7 | 13.7 | 0.1 | 13.8 | 108.8 |
| Pyridyl-S-Sepharose 6 FF | 6.7 | 6.4 | 0.0 | 6.4 | 96.0 |
| Butyl-S-Sepharose 6 FF | 3.6 | 4.1 | 0 | 4.1 | 112.4 |
| Butyl Sepharose HP | 13.5 | 13.7 | 0 | 13.7 | 101.5 |
| Source 15 PHE | 12.1 | 9.6 | 2.2 | 11.8 | 98.0 |
| Source 15 ISO | 1.9 | 2.1 | 0 | 2.1 | 110.8 |
| BSA 1.75 M | | | | | |
| Phenyl Sepharose HP | 23.3 | 20.3 | 2.9 | 23.2 | 99.6 |
| Phenyl Sepharose high sub | 13.5 | 11.2 | 1.7 | 12.9 | 95.6 |
| Phenyl Sepharose low sub | 11.5 | 10.6 | 0.2 | 10.8 | 94.0 |
| Butyl Sepharose 4 FF | 8.2 | 8.3 | 0.1 | 8.4 | 101.9 |
| Octyl Sepharose FF | 13.7 | 13.1 | 0.4 | 13.5 | 98.5 |
| Toyopearl Butyl 100 μm | 8.0 | 6.5 | 1.1 | 7.6 | 95.0 |
| Hexyl-S-Sepharose 6 FF | 44.0 | 46.1 | 0.7 | 46.8 | 106.3 |
| Methyl Sepharose 4 FF | 33.0 | 31.7 | 0.1 | 31.8 | 96.3 |
| Pyridyl-S-Sepharose 6 FF | 37.9 | 30.9 | 0.1 | 31.0 | 81.8 |
| Butyl-S-Sepharose 6 FF | 41.0 | 39.9 | 0.26 | 40.16 | 98.0 |
| Butyl Sepharose HP | 40.3 | 44.9 | 0.3 | 45.2 | 112.2 |
| Macroprep methyl | 10.9 | 6.6 | 0.0 | 10.3[b] | 94.5 |
| Macroprep *t*-butyl | 2.6 | 1.6 | 0.2 | 2.7[c] | 103.1 |
| Source 15 PHE | 12.1 | 12.8 | 1.5 | 14.3 | 119.0 |
| Source 15 ISO | 11.2 | 10.0 | 0.1 | 10.1 | 90.2 |
| Toyopearl Hexyl 100 μm | 22.0 | 12.6 | 9.2 | 21.8 | 99.0 |
| Ovalbumin 1.5 M | | | | | |
| Phenyl Sepharose HP | 6.2 | 6.6 | 0.2 | 6.8 | 110.2 |
| Phenyl Sepharose high sub | 9.0 | 7.4 | 0 | 7.4 | 82.2 |
| Phenyl Sepharose low sub | 10.0 | 8.3 | 0 | 8.3 | 83.0 |
| Butyl Sepharose 4 FF | 6.0 | 4.8 | 0 | 4.8 | 80.0 |
| Octyl Sepharose 4FF | 10.0 | 8.5 | 0 | 8.5 | 85.0 |
| Toyopearl Butyl 100 μm | 7.0 | 6.8 | 0.5 | 7.3 | 103.0 |
| Hexyl-S-Sepharose 6 FF | 2.94 | 2.62 | 0.03 | 2.65 | 90.1 |

Table 3. Continued

| | Total protein (mg) | Eluate (mg) | Regenerate (mg) | Recovered protein (mg) | Total recovery (%) |
|---|---|---|---|---|---|
| Methyl Sepharose 4 FF | 6.3 | 5.5 | 0.04 | 5.54 | 87.9 |
| Pyridyl-S-Sepharose 6 FF | 15.4 | 12.7 | 0.03 | 12.73 | 82.9 |
| Butyl-S-Sepharose 6 FF | 1.75 | 1.05 | 0 | 1.35[d] | 77.0 |
| Butyl Sepharose HP | 10.0 | 8.4 | 0.1 | 8.5 | 84.6 |
| Macroprep methyl | 3.0 | 2.6 | 0.1 | 2.7 | 88.3 |
| Toyopearl Hexyl 100 μm | 14.0 | 13.2 | 1.2 | 14.4 | 103.0 |
| Ovalbumin 1.75 M | | | | | |
| Phenyl Sepharose HP | 19.2 | 15.3 | 0.1 | 15.4 | 80.3 |
| Phenyl Sepharose high sub | 12.7 | 11.5 | 0.1 | 11.6 | 90.9 |
| Phenyl Sepharose low sub | 10.3 | 10.3 | 0.1 | 10.4 | 100.6 |
| Butyl Sepharose 4 FF | 7.7 | 7.3 | 0.1 | 7.4 | 95.6 |
| Octyl Sepharose FF | 12.8 | 11.0 | 0.1 | 11.1 | 87.0 |
| Toyopearl Butyl 100 μm | 12.0 | 10.2 | 0.4 | 10.6 | 88.3 |
| Hexyl-S Sepharose 6 FF | 10.7 | 10.2 | 0 | 10.2 | 95.3 |
| Methyl Sepharose 4 FF | 12.6 | 10.3 | 0.2 | 10.5 | 83.3 |
| Pyridyl-S-Sepharose 6 FF | 28.0 | 21.9 | 0.2 | 22.1 | 78.9 |
| Butyl-S-Sepharose 6 FF | 8.0 | 9.1 | 0 | 9.1 | 113.8 |
| Butyl Sepharose HP | 37.7 | 32.1 | 0.7 | 32.8 | 87.0 |
| Source 15 Phenyl | 16.8 | 16.0 | 0.2 | 16.2 | 96.3 |
| Source 15 ISO | 18.2 | 19.4 | 0.1 | 19.5 | 107.1 |
| Macroprep methyl | 3.2 | 3.9 | 0.1 | 4.0 | 127.0 |
| Toyopearl Hexyl 100 μm | 25.0 | 21.2 | 0.4 | 21.6 | 86.0 |

[a] 0.72 mg were found in the wash out.
[b] 3.7 mg were found in the wash out.
[c] 0.9 mg were found in the wash out.
[d] 0.3 mg were found in the wash out.

approach remains a compromise, since currently there is no method available to measure hydrophobicity in porous chromatography media.

## 5. Nomenclature

| | |
|---|---|
| $d_p$ | particle diameter (cm) |
| $D_L$ | axial dispersion coefficient ($cm^2/s$) |
| $D_m$ | molecular diffusivity in free solution ($cm^2/s$) |
| $D_p$ | pore diffusivity ($cm^2/s$) |
| $D_s$ | surface diffusivity ($cm^2/s$) |
| $N$ | number of plates |
| $h$ | reduced HETP |
| $k'$ | retention factor |
| $k_f$ | film mass transfer coefficient (cm/s) |
| $k_p$ | pore diffusion mass transfer coefficient (cm/s) |
| $K$ | partition coefficient |
| $q$ | adsorbed protein (mg) |
| $r_p$ | particle radius (cm) |
| $r_s$ | radius of subparticle (cm) |
| $u$ | linear flow velocity (cm/s) |
| ReSc | dimensionless velocity |
| $\epsilon$ | void fraction |
| $\epsilon_p$ | particle porosity |
| $\rho_p$ | particle density (g/ml) |
| $\sigma$ | standard deviation |

## Acknowledgements

The financial support of Amersham Biosciences is greatly acknowledged.

## References

[1] C.C. Shepard, A. Tiselius, in: Discussion of the Faraday Society, Hazell Watson and Winey, London, 1949, p. 275.

[2] M.T. Hearn, in: S. Ahuja (Ed.), Handbook of Bioseparation, Academic Press, New York, 2000, pp. 71–235.
[3] J.A. Queiroz, C.T. Tomaz, J.M.S. Cabral, J. Biotechnol. 87 (2001) 143.
[4] A. Berggrund, I. Drevin, K.-G. Knuuttila, J. Wardhammar, B.-L. Johansson, Proc. Biochem. 29 (1994) 455.
[5] E. Boschetti, A. Jungbauer, in: S. Ahuja (Ed.), Handbook of Bioseparation, Academic Press, New York, 2000, pp. 535–632.
[6] J.-C. Janson, L.E. Ryden, Protein Purification, 2nd ed, Wiley–VCH, New York, 1998, p. 283.
[7] G. Halperin, M. Breitenbach, M. Tauber-Finkelstein, S. Shaltiel, J. Chromatogr. 215 (1981) 211.
[8] J.-L. Ochoa, Biochimie 60 (1978) 1.
[9] S. Hjerten, J. Mohammad, K.O. Eriksson, J.L. Liao, Chromatographia 31 (1991) 85.
[10] H.P. Jennissen, A. Demiroglou, J. Chromatogr. 597 (1992) 93.
[11] T.W. Hutchens, J. Porath, Anal. Biochem. 159 (1986) 217.
[12] W. Schwart, D. Judd, M. Wysocki, L. Guerrier, E. Birck-Wilson, E. Boschetti, J. Chromatogr. A 908 (2001) 251.
[13] P.P. Berna, N. Berna, J. Porath, S. Oscarsson, J. Chromatogr. A 800 (1998) 151.
[14] M.T.W. Hearn, in: K.M. Gooding, F.E. Regnier (Eds.), HPLC of Biological Macromolecules, Marcel Dekker, New York, 2002, p. 99.
[15] A. Jungbauer, W. Feng, in: K.M. Gooding, F.E. Regnier (Eds.), HPLC of Biological Macromolecules, Marcel Dekker, New York, 2002, pp. 281–373.
[16] W.R. Melander, Cs. Horváth, Arch. Biochem. Biophys. 183 (1977) 200.
[17] W.R. Melander, C. Horvát, J. Chromatogr. 317 (1984) 67.
[18] A. Tongta, A.I. Liapis, D.J. Siehr, J. Chromotgr. A 686 (1994) 21.
[19] J.R. Conder, B.O. Hayek, Biochem. Eng. J. 6 (2000) 215.
[20] J.L. McNay, E.J. Fernandez, J. Chromatogr. A 849 (1999) 135.
[21] P. Kaarsnaes, T. Lindblom, J. Chromatogr. 599 (1992) 131.
[22] Q.M. Mao, I.G. Prince, M.T.W. Hearn, J. Chromatogr. A 646 (1993) 81.
[23] C. Machold, K. Deinhofer, R. Hahn, A. Jungbauer, J. Chromatogr. A 972 (2002) 3.
[24] D.U. Rosenberg, AIChE J. 2 (1956) 55.
[25] H.P. Lettner, O. Kaltenbrunner, A. Jungbauer, J. Chromatogr. Sci. 33 (1995) 451.
[26] M.D. LeVan, G. Carta, C.M. Yon, in: D.W. Green (Ed.), Perry's Chemical Engineers Handbook, McGraw-Hill, New York, 1997.
[27] T.K. Sherwood, R.L. Pigford, C.R. Wilke, Mass Transfer, McGraw-Hill, New York, 1975.
[28] H.C. Thomas, J. Am. Chem. Soc. 66 (1944) 1664.
[29] E. Hansen, PhD thesis, Departement of Chemical Engineering, Technical University of Denmark, DTU, Lyndby, Denmark 2000.
[30] D. Corradini, D. Capitani, L. Cellai, J. Liq. Chromatogr. 17 (1994) 4335.
[31] A. Staby, J. Mollerup, J. Chromatogr. A 734 (1996) 205.
[32] K. Benedek, J. Chromatogr. 458 (1988) 93.